**Yasuyuki Tokumitsu** (M'79) was born in Shimonoseki, Japan, on May 15, 1943. He received the B.E. and M.E. degrees from Kyushu Institute of Technology, Kitakyushu, Japan, in 1966 and 1968, respectively.

In 1968 he joined Fujitsu Laboratories, Ltd., Kawasaki, Japan, where he has been engaged in the research and development of passive and active components for microwave communication equipment. Currently, he is interested in millimeter-wave hybrid integrated circuits, millimeter-wave radio communication equipment, and satellite communication equipment. He is now leading the Radio and Satellite Communications System Components Development Group in the Radio and Satellite Communications Systems Laboratory of Fujitsu Laboratories Ltd.

Mr. Tokumitsu is a Member of the Institute of Electronics and Communication Engineers of Japan.

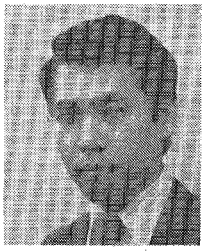

**Masayuki Ishizaki** was born in Yokohama, Japan, on Oct. 18, 1951. He was graduated from the electrical engineering department of Kanagawa Technical High School, Yokohama, Japan, in 1970, and Fujitsu Technical College in 1974.

He joined Fujitsu Laboratories Ltd., Kawasaki, Japan, in 1970, and has been engaged in the research and development of microwave integrated circuits and millimeter waveguide components for a guided millimeter-wave transmission system. He is presently engaged in the research and development of millimeter-wave radio communication equipment, and is an Engineer at the Radio and Satellite Communications Systems Laboratory in Fujitsu Laboratories Ltd.

Mr. Ishizaki is a Member of the Institute of Electronics and Communication Engineers of Japan.

**Mikio Iwakuni** was born in Hyogo, Japan, on December 8, 1953. He was graduated from the electrical engineering department of Himeji Technical High School, Japan, in 1972, and Fujitsu Technical College in 1976.

He joined Fujitsu Laboratories Ltd., Kawasaki, Japan, in 1972, and has been engaged in the research and development of microwave system components for radio communication systems, mainly solid-state sources. He is now an Engineer at the Radio and Satellite Communications Systems Laboratory, Integrated Communications Division, Fujitsu Laboratories Ltd.

Mr. Iwakuni is a member of the Institute of Electronics and Communications Engineers of Japan.

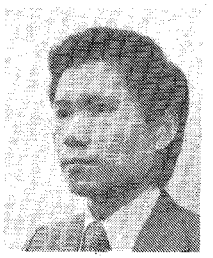

**Toshiyuki Saito** was born in Mie, Japan, on August 11, 1945. He received the B.S. degree from Tokyo Denki University, Tokyo, in 1970, and the M.S. degree from Chiba University, Chiba, Japan, in 1972.

In 1972 he joined Fujitsu Laboratories Ltd., Kawasaki, Japan, where he has been engaged in the research and development of microwave system components for radio communication systems, mainly solid-state components, and microwave and millimeter-wave integrated circuits. He is now a Senior Engineer at the Radio and Satellite Communications Systems Laboratory, Integrated Communications Division, Fujitsu Laboratories Ltd.

Mr. Saito is a member of the Institute of Electronics and Communication Engineers of Japan.

# Design of Dielectric Ridge Waveguides for Millimeter-Wave Integrated Circuits

TAICHI WANG, STUDENT MEMBER, IEEE, AND S. E. SCHWARZ, SENIOR MEMBER, IEEE

*Abstract*—**All-dielectric ridge waveguides may be useful as elements of millimeter- and submillimeter-wave integrated circuits. A planar metallic V-coupler can be used to couple energy between the guide and small circuit elements such as diodes. Desirable characteristics in such a guide/coupler system are: a) quasi-single mode propagation; b) low radiation loss in bends; c) low coupling loss between guide and devices; and d) adequate physical strength. In this paper, we discuss the general problem of designing guides and couplers to obtain the desired characteristics. The principal method used is simulation in the range 2–7 GHz. We find that with good compromise designs, typical coupling loss between waveguide and a small device is about 1.4 dB, exclusive of dielectric loss and ohmic loss in the coupler.**

Manuscript received March 9, 1982; revised May 27, 1982. This work was supported by the National Science Foundation under Grant ECS-7813933, the Joint Services Electronics Program under AFOSR Contract F49620-79-C-0178, the U.S. Army Research Office under Contract DAAG29-79-C-0134, and the U.S. Army under MERADCOM Grant DAAK70-80-C-013A.

The authors are with the Department of Electrical Engineering and Computer Sciences and the Electronics Research Laboratory of the University of California, Berkeley, CA 94720.

## I. Introduction

DIELECTRIC waveguides are potentially useful alternatives to metallic guides at high frequencies, where metallic conduction losses become excessive. Various kinds of dielectric waveguides, such as rectangular waveguide [1], [2], image guide [3]–[5], strip guide [6], [7], inverted strip guide [8], [9], and trapped image guide [10] have been proposed and analyzed. A general method for analyzing

0018-9480/83/0200-0128$01.00 ©1983 IEEE

this class of open dielectric waveguides has recently been proposed [11], [12]. Those guides that are made entirely of dielectric (and do not use metal image planes) are of course free of metallic loss, except for losses in small metallic coupling structures. Their loss advantage over metallic guides tends to increase with increasing frequency. For the all-dielectric guides, an upper bound of the power attenuation coefficient is the bulk attenuation coefficient $\alpha = \sigma\sqrt{\mu/\epsilon}$, where $\sigma$, $\mu$, and $\epsilon$ are the conductivity, magnetic permeability, and electric permittivity of the dielectric, respectively. Assuming that the conductivity of the dielectric is independent of frequency $f$, $\alpha$ is also independent of frequency and the loss per guide wavelength decreases as $1/f$. For metallic waveguides, on the other hand, two effects cause the loss per guide wavelength to increase with frequency: the dimensions become smaller in proportion to $1/f$, and the surface resistance increases in proportion to $\sqrt{f}$. Thus, typically, the ratio of the loss per guide wavelength for a dielectric guide to that of a metallic guide is on the order of $(f_1/f)^{3/2}$, where $f_1$ is a crossover frequency determined by the details of the guides in question. (Let the metallic guide be a 50-Ω microstrip made of copper on a BeO substrate with substrate thickness $h = \lambda_0/20$, where $\lambda_0$ is the free-space wavelength, and let the ratio of the copper thickness to the substrate thickness be 1 : 10. Using the above-mentioned upper bound to approximate the loss of a 1000-Ω·cm silicon dielectric waveguide, we find a crossover frequency of 67 GHz.) When the material of the dielectric guide is a semiconductor, it becomes possible to fabricate semiconductor devices in the same piece of material [3], [13]. In the near-millimeter regime, dimensions of quasi-single-mode waveguides are convenient for fabrication by photolithography.

In this paper, the design of one particular type of all-dielectric waveguide, the dielectric ridge guide (DRG, see Fig. 1) is considered. The reasons for choosing this particular guide have to do with its potential application as a component of near-millimeter-wave integrated circuits (NMIC). a) The shape can be conveniently etched out of semiconductor wafers. The web isolates the guided field from other components on the wafer while providing structural support. b) Ohmic losses (such as those associated with dielectric image guide) are avoided. c) A convenient method exists for coupling radiation into the guide. This can be done by tapering the end of the guide into a dielectric antenna. Patterns obtained in this way are single-lobed and nearly symmetrical with gain on the order of 10 dB [14]. The most promising technique for fabrication appears to be anisotropic etching of semiconductors. With this technique, the cross section of the guide is not rectangular, but rather trapezoidal with an angle $\alpha$ determined by the crystal structure. (For silicon, $\alpha = 55°$.)

In the NMIC, there can be several devices, active or passive, distributed or lumped, interconnected by dielectric waveguide. For small lumped elements, such as diodes, a way must be found to couple energy efficiently between the waveguide and the device. At lower frequencies, this can be done by inserting a tapered section of waveguide into a hollow metallic waveguide, where the device can then be mounted on a post. In a monolithic NMIC, where metal waveguide is to be avoided, it is convenient to use the planar V-coupler of Rutledge *et al.* [14]. This consists of a metallic V-shaped structure deposited on the back (planar) surface of the dielectric wafer, where its fields interact with those of the guide. The device to be coupled is connected at the vertex of the V.

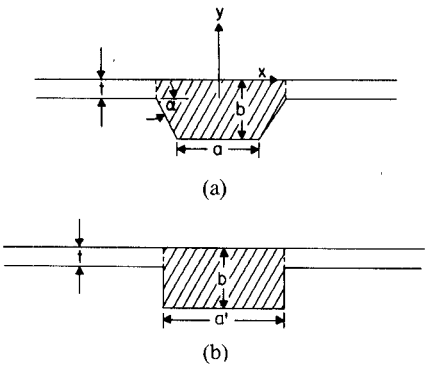


Fig. 1. The dielectric ridge guide (DRG). (a) A DRG fabricated in semiconductor by anisotropic etching; for silicon, $\alpha = 55°$. (b) Equivalent rectangular DRG used in the EDC method to approximate the trapezoidal DRG.

A principal objective in the design of DRG and V-coupler is efficient coupling between the guide and the small device at the vertex of the V. It is also desirable to reduce radiation from the guide; although little radiation occurs in unperturbed straight sections, energy will be lost into slab modes of the support web whenever there is a discontinuity or bend. Further considerations are structural strength and ease of fabrication; the support web should therefore not become too thin. Finally, we shall require quasi-single-mode propagation, in the sense that at the operating frequency, only the non-leaky wave and the lowest order leaky wave propagates. In Section II, we shall discuss the design of the guide itself, using the well-known effective dielectric constant (EDC) method as our principal tool for analysis. In Section III, design of the V-coupler will be considered. Design data are based primarily on simulation at 2–7 GHz.

## II. The Dielectric Ridge Guide

The DRG consists of a central guiding region of width $a$ and height $b$ supported by a web of thickness $t$, as shown in Fig. 1(a). A general and exact method for obtaining a complete description of the guided modes of the DRG has recently been published [11], [12]. By convention, the guided modes of the DRG can be classified according to their dominant electric field direction. The mode designated $E^x_{pq}$ is one with dominant electric field in the $x$-direction and with $p$ and $q$ field maxima in the $x$- and $y$-directions, respectively; similarly for $E^y_{pq}$ modes. The DRG can support two fundamental modes, the $E^x_{11}$ and $E^y_{11}$ modes. These two modes are propagating for all choices of guide dimensions. As pointed out by Peng and Oliner [11], [12], all modes are leaky except for the $E^x_{11}$ mode. In the present work, the operative mode is assumed to be $E^x_{11}$, and guide dimensions are chosen such that all the other modes except $E^y_{11}$ are cut off.

In some circumstances, only the propagation constant is needed. In this case, the effective dielectric constant (EDC) method [3] is a convenient approximate method which is known to give fairly accurate results. In order to gain understanding of the nature and limitations of the EDC method, we can relate the EDC method to Peng and Oliner's formalism. In their building-block approach, the cross-sectional geometry of the rectangular DRG is first broken into three constituent parts; a rectangular core region of thickness $b$ is supported by two web regions of thickness $t$. Since the TE and TM modes of a slab together form a complete set of functions, the guided mode in the core region can be decomposed into a summation of slab modes for a slab with the height of the core, and similarly the portion of the guided mode in the web region can be decomposed into a summation of slab modes for a slab the height of the web. The propagation constants are obtained by requiring that the fields of the guided mode satisfy the transverse resonance condition. Let $\phi_n'$ and $\phi_m''$ denote the transverse-mode functions of the $n$th TE and $m$th TM slab modes in the core region, respectively, for $n, m = 1,2,3,\cdots$, and let $k_n'$, $k_m''$ and $n_n'$, $n_m''$ be the propagation constants and effective indices of refraction of the corresponding slab modes where

$$n_n' \equiv \frac{k_n'}{k_0}, \qquad n_n'' \equiv \frac{k_n''}{k_0}$$

and $k_0$ = propagation constant in free space. Similarly, the transverse-mode functions, propagation constants, and effective indices of refraction can be defined for the web regions; they are denoted by the corresponding barred quantities, $\bar{\phi}_n'$, $\bar{\phi}_m''$, $\overline{k_n'}$, $\overline{k_m''}$, and $\overline{n_n'}$, $\overline{n_m''}$. Carrying through the transverse resonance analysis to obtain an approximate solution, the expansions are truncated to retain only the lowest order TE slab modes, and we obtain the following expression for the propagation constant $k_z$ of the $E_{11}^x$ mode:

$$\left[n_1'^2 k_0^2 - k_z^2\right]^{1/2} a = \pi - 2\tan^{-1} \times \left[\left(\frac{\overline{n_1'}}{n_1'}\right)^2 \frac{\left[(n_1')^2 k_0^2 - k_z^2\right]^{1/2}}{\left[k_z^2 - \left(\overline{n_1'}\right)^2 k_0^2\right]^{1/2} H}\right] \quad (1)$$

where

$$H = \frac{|\langle \bar{\phi}' | \phi' \rangle|^2}{\langle \bar{\phi}' | \bar{\phi}' \rangle \langle \phi' | \phi' \rangle} \quad (2)$$

and

$$\langle f | g \rangle \equiv \int_{-\infty}^{\infty} f(y) g(y)\, dy.$$

If we set $H = 1$, we obtain the same expression as is given by the EDC method. Since the effective indices of refraction appearing in (1) are those of the lowest order TE slab mode, they satisfy

$$\left[\epsilon_r - n^2\right]^{1/2} k_0 l = \pi - 2\tan^{-1}\left(\frac{\epsilon_r - n^2}{n^2 - 1}\right)^{1/2} \quad (3)$$

where $\epsilon_r$ is the relative dielectric constant of the waveguide material, and $n = n'$, $l = b$, and $n = \overline{n'}$, $l = t$ for the slab modes in the core and web regions, respectively. Thus, the EDC method is expected to be accurate when the contribution from the higher order slab modes is small so that (1) is accurate and $H \simeq 1$. This will be the case when $(b - t)/b \ll 1$. Moreover, the EDC method becomes more accurate as $b$ decreases, because the contribution of the lowest order mode increases with decreasing slab height.

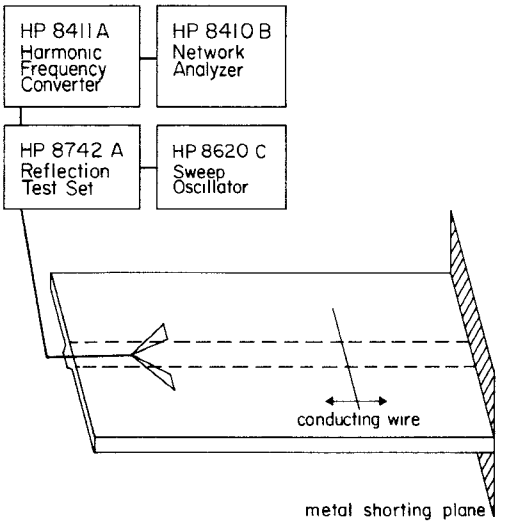


Fig. 2. Experimental setup used in dispersion measurement.

A quantity of interest is the cutoff frequency of the next higher order mode. In the EDC approximation cutoff of the $E_{21}^x$ mode occurs when

$$a = \frac{\lambda_0}{2\left[n'^2 - \overline{n'}^2\right]^{1/2}}. \quad (4)$$

For the $E_{12}^x$ mode, cutoff occurs when

$$b = \frac{\lambda_0}{2[\epsilon_r - 1]^{1/2}}. \quad (5)$$

Although the EDC method is widely used, experimental confirmations have been obtained either for multimode waveguides or for guides in which the differences of dielectric constant between the guide and its surroundings were small [3], [5], [15]. We have carried out a simulation experiment in the frequency range 2–7 GHz to verify the EDC method in the quasi-single-mode regime. Emerson and Cuming Hi$K$ material with $\epsilon_r = 12$ is used to simulate silicon waveguide at millimeter wavelengths. The trapezoidal core region can be represented by an effective rectangular core region of the same height and core area whose width is $a'$, as shown in Fig. 1(b). The experimental setup is shown in Fig. 2. Power from the sweep oscillator is coupled into the DRG by a V-coupler. A shorting plane at the far end of the waveguide establishes a standing wave. The reflected wave is coupled back into the coaxial cable by the V-coupler. The magnitude and phase of the reflected wave are then measured by the network analyzer. When a small conducting wire is placed near the waveguide, the reflected wave is disturbed, except when the wire is located at one of the nodes of the field parallel to the probe. Thus, the guide wavelength is measured by locating the nodes.

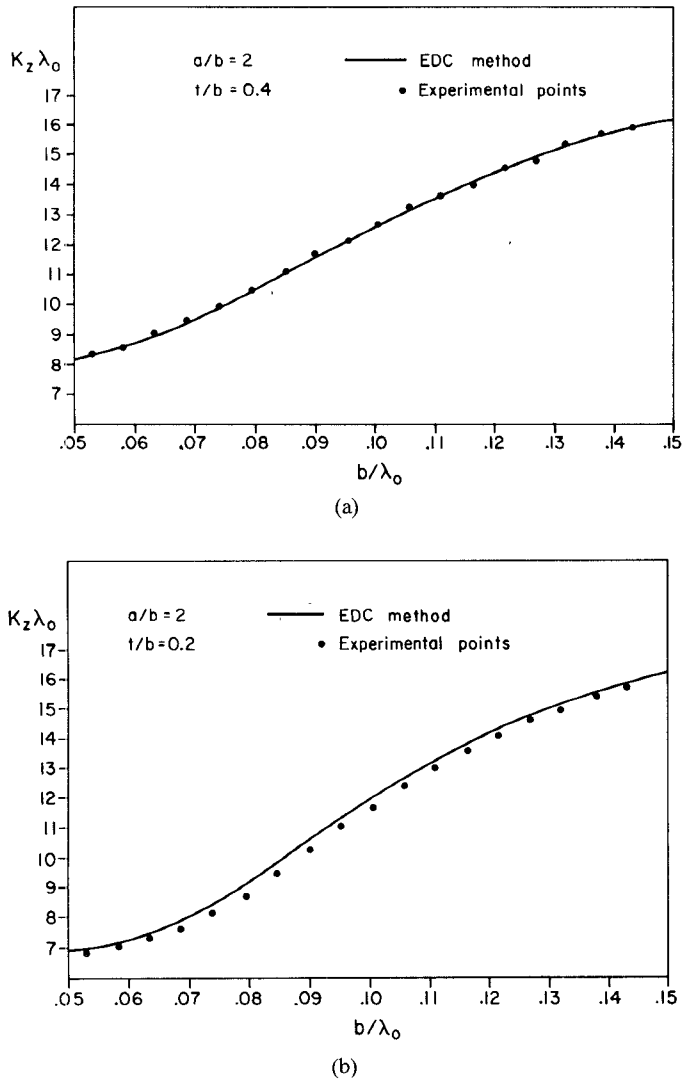


Fig. 3. Comparison of the measured dispersion curves (experimental points) with those predicted by the EDC method (solid line) for DRG with $a/b = 2$. (a) $t/b = 0.4$. (b) $t/b = 0.2$.

In Fig. 3, the measured propagation constant is plotted against normalized guide height $b/\lambda_0$ for guides with $a/b = 2$, for the two cases $t/b = 0.2$ and 0.4. Also shown in the figure are the dispersion curves predicted by the EDC method. We see that the propagation constant is predicted quite well by the EDC method for $t/b = 0.4$. In this case, the error is less than 4 percent over the range of measurement. However, for $t/b = 0.2$, errors become more significant. As was discussed before, in general the EDC method becomes more accurate for larger values of $a/b$ and $t/b$.

Having verified the accuracy of the EDC method for cases of interest, we can now use it to design the waveguide. There are several considerations that will affect our choice of waveguide geometry: a) all the higher order modes are to be cut off; b) reasonably small radii of curvature should give tolerable radiation loss; c) coupling loss between waveguide and V-coupler should be acceptably small; and d) the web thickness should be thick enough to provide adequate physical strength. The first of these considerations has already been dealt with. We shall discuss b), c), and d) in the following paragraphs.

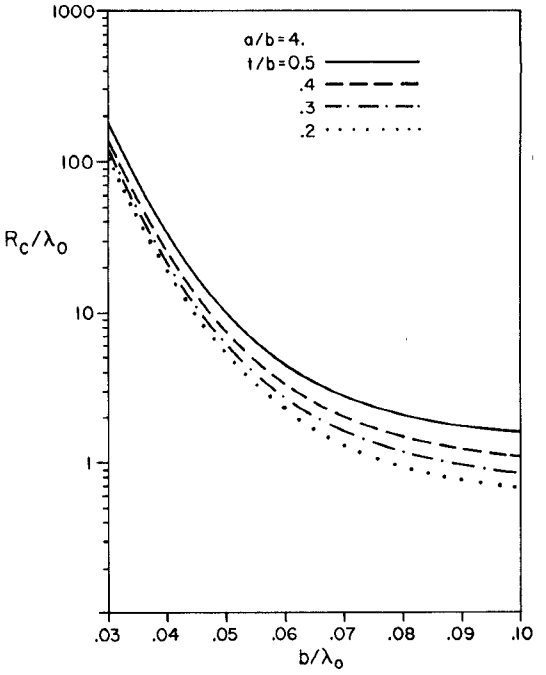


Fig. 4. Critical radius of curvature $R_c$ from (8) for DRG with $a/b = 4$.

All open waveguide structures suffer from radiation loss when the guide is curved. From a general analysis of the directivity of electromagnetic waves, it has been shown that the dominant dependence of the radiation loss on the radius of curvature $R$ is of exponential nature [16], [17]. When $R$ is larger than a critical radius of curvature $R_c$, the radiation loss decreases very slowly with increasing $R$. On the other hand, when $R$ is smaller than $R_c$, radiation loss increases very rapidly as $R$ decreases. The critical radius of curvature is given approximately by

$$R_c = 6k_z^2\xi_t^3 \tag{6}$$

where $k_z$, the propagation constant in the curved section, can be approximated by that in the straight guide, and $\xi_t$ is the decay length of the fields in the web region. We can estimate $\xi_t$ by using the decay length of the lowest order TE slab mode given by

$$\xi_t = \left[k_z^2 - \overline{n'}^2 k_0^2\right]^{-1/2}. \tag{7}$$

This is a good approximation because the guided mode is a superposition of the slab modes and for the $E_{11}^x$ mode, the dominant contribution is from the lowest order TE slab mode. Furthermore, the field components of the higher slab modes extend less far into the web, and thus make a smaller contribution to the radiation loss. The exponential nature of the dependence of radiation loss on $R$ and the validity of (6) have been verified in [18]. (Actually the critical radius of curvature verified in [18] is $2k_z^2\xi_t^3$. The numerical constant in (6) is of course somewhat arbitrary. We adopt the factor of 6 used by Marcatili [16] as being more conservative.) It is reasonable to consider the minimum usable radius of curvature of a curved section to be on the order of $R_c$. The calculated values of $R_c$ for $a/b = 4$ as a function of normalized guide height $b/\lambda_0$ for several values of $t/b$ are shown in Fig. 4. It is seen that $R_c$

increases rapidly as $t/b$ changes from 0.4 to 0.5 while it remains about the same for $t/b$ smaller than 0.4. Calculations for $a/b = 2$ lead to a similar conclusion. In order to have a thick web for the sake of mechanical strength, $t/b = 0.4$ is a logical choice.

The only variable left for the DRG design is the ratio $a/b$. In order for the higher order modes to be cut off, the product $ab$ must not be too large. Thus, smaller $a$ implies larger $b$, and since $t/b$ has been fixed, larger $t$ as well. Thus, greater mechanical strength is obtained with a smaller value of $a/b$. For the web to be thicker than 75 $\mu$m, at 100 GHz, $a/b$ has to be smaller than 4.5. As $a/b$ becomes smaller, however, the fields are less confined in the $x$-direction and this leads to more radiation loss from a curved section with the critical radius of curvature. Thus, choice of $a/b$ amounts to a compromise between mechanical strength and reduction of radiation loss from curved sections. In order not to unduly increase the radiation loss, $a/b \geq 2$ has been chosen. In order to choose a value of $a/b$ within the range $2 \leq a/b \leq 4.5$, we must consider the influence of this parameter on the coupling loss between the guide and V-coupler.

## III. The V-Coupler

A V-coupler with inner angle $\theta$, angular arm width $\Delta\theta$, and length $l$ is shown in Fig. 5. The V-coupler is characterized by a driving-point impedance $Z$ and coupling loss $L$. The design value of $Z$ will be 100 Ω. The objective of the design of the V-coupler and the DRG (with $t/b = 0.4$) is to find values of $\theta$, $\Delta\theta$, $l$, and $a/b$ that result in minimum coupling loss.

In earlier work [14], [19], an approximate formula for the V-coupler's driving point impedance was used

$$Z = \frac{377\ \Omega}{\sqrt{\frac{\epsilon_r + 1}{2}}} \frac{K(k)}{K\left(\sqrt{1-k^2}\right)} \tag{8}$$

where $K$ is the complete elliptic integral of the first kind and

$$k = \frac{\tan\frac{\theta}{2}}{\tan\frac{\theta + \Delta\theta}{2}}. \tag{9}$$

This formula is based on conformal mapping of coplanar strips in free space. The correction factor

$$\sqrt{\frac{\epsilon_r + 1}{2}}$$

is used to take into account the presence of the dielectric waveguide [20]. This formula was shown to give estimates of $Z$ to within 30 percent for rectangular and trapezoidal dielectric waveguides without webs [14], but our simulation experiments indicate that it is not a good approximation for V-couplers on DRG. The operation of the V-coupler involves radiation into free space, coupling to the slab modes, and ohmic loss. A complete description would require a full wave analysis, which is still lacking. The approach we have used is to design by means of simulation in the frequency range 2–6 GHz.

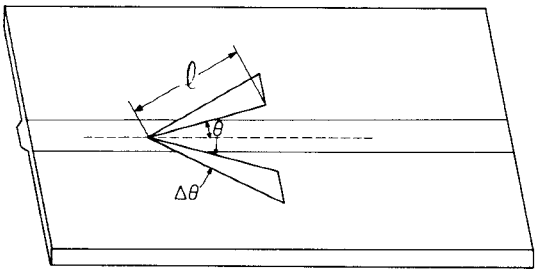


Fig. 5. The V-coupler.

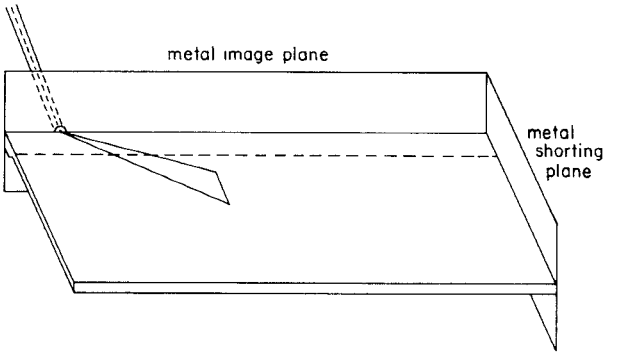


Fig. 6. Experimental setup used in the V-coupler design. The electronics are the same as in the dispersion measurement.

The experimental setup is shown in Fig. 6. The V-coupler is cut from 3-mil copper foil. An image plane is used in the simulation in order to avoid a balun between asymmetric coax and the symmetric V-coupler. The image plane reduces the observed driving-point impedance by half. When the waveguide is terminated by a good absorber, the network analyzer measures the driving-point impedance of the V-coupler. Once the driving-point impedance has been adjusted to 50 Ω (with image plane; 100 Ω without image plane), the network analyzer then measures the two-way coupling loss. (The measurement actually also includes whatever dielectric loss and scattering loss exist in waveguide. These, however, are expected to be small and, in any case, do not affect minimization of the coupling loss.)

It is found experimentally that the driving-point impedance of the V-coupler does not vary much with the length of its arms, so long as $l\sin\theta \gtrsim 0.7a$. The experimental procedure is to find a set of $\{\theta, \Delta\theta\}$ that gives the correct driving-point impedance for a long V-coupler on a given DRG. We find that typically a driving point reflection coefficient of less than $-18$ dB can be obtained over a 10 percent bandwidth. Because we are interested primarily in the frequencies just below the cutoff frequency $f_{21}$ of the $E_{21}^x$ mode (the next higher order mode for DRG with $t/b = 0.4$ and $a/b \geq 2$), the design is adjusted to give reflection coefficient $< 18$ dB over approximately the range $0.9f_{21} < f < f_{21}$.

Although (8) is not itself a good approximation, it is found that the set of designs $\{\theta, \Delta\theta\}$ giving the correct driving-point impedance is characterized by a constant value of the constant $k$ defined in (9). This means that once

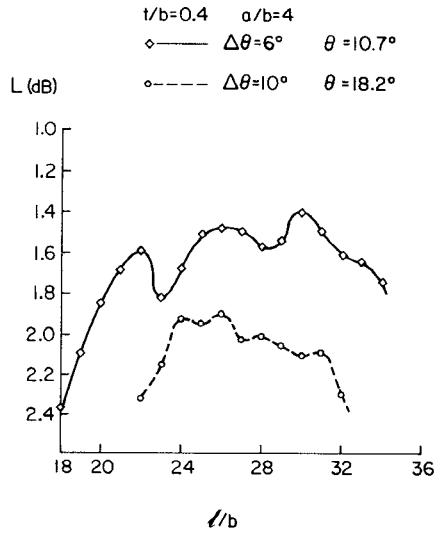


Fig. 7. Typical coupling loss $L$ as a function of coupler length $l$.

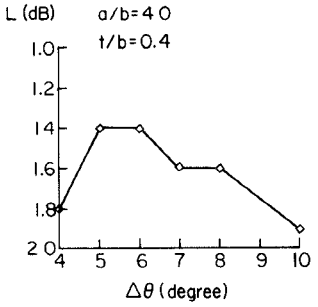


Fig. 8. Coupling loss as a function of $\Delta\theta$ (with $l$ always adjusted for lowest loss) for V-couplers on DRG with $a/b = 4$. The values of $\theta$ are given in Table I.

a pair of angles $\theta, \Delta\theta$ is found that gives the desired impedance, other pairs of angles resulting in the same value of $k$ will also give that impedance. Thus, by modifying the constant factor in (8), an approximate formula for $Z$ may be obtained. The formula

$$Z \simeq \frac{377\ \Omega}{n' + \overline{n'}} \frac{K(k)}{K\left(\sqrt{1-k^2}\right)} \tag{10}$$

is found to be accurate within 15 percent, where $\overline{n'}$ and $n'$ are the effective indices of refraction at $f = 0.95 f_{21}$.

Once $\theta$ and $\Delta\theta$ have been found, the coupling loss is measured as a function of coupler length and frequency. The measured coupling loss usually varies $\pm 0.2$ dB over the frequency range of interest; thus, in comparing designs we actually compare typical values of the loss $L$. A plot of $L$ as a function of coupler length on waveguide with $a/b = 4$ for two pairs of angles $\theta, \Delta\theta$ (both of which give the desired driving-point impedance), is shown in Fig. 7. The coupling loss as a function of $\Delta\theta$ (with $l$ always adjusted for lowest loss), for V-couplers on DRG with $a/b = 4$, is shown in Fig. 8. The corresponding designs are shown in Table I. The best design for $a/b = 4$ is found to be $\theta = 9°$, $\Delta\theta = 5°$, $l = 28b$. In this case, the coupling loss is 1.4 dB. The above procedures can be repeated for DRG's with different $a/b$, in order to obtain an overall design of

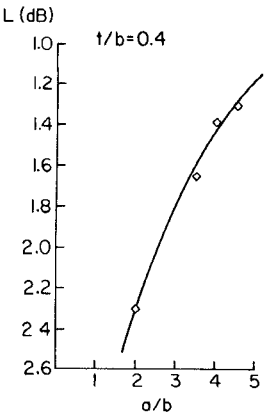


Fig. 9. The minimum coupling loss achievable as a function of $a/b$. The values of $\Delta\theta, \theta, l$ are given by Table II.

TABLE I
DATA FOR EXPERIMENTAL POINTS SHOWN IN FIG. 8

| a/b = 4, t/b = 0.4 | | | |
|---|---|---|---|
| Δθ | θ (deg) | ℓ/b | L(dB) |
| 4 | 7.1 | 30 | 1.8 |
| 5 | 8.9 | 28 | 1.4 |
| 6 | 10.7 | 30 | 1.4 |
| 7 | 12.5 | 28 | 1.6 |
| 8 | 14.4 | 27 | 1.6 |
| 9 | 16.2 | -- | --- |
| 10 | 18.2 | 26 | 1.9 |

TABLE II
DATA FOR EXPERIMENTAL POINTS SHOWN IN FIG. 9

| t/b = 0.4 | | | | | |
|---|---|---|---|---|---|
| a/b | k | Δθ(deg) | θ(deg) | ℓ/b | L(dB) |
| 2 | .707 | 6° | 15° | 13 | 2.3 |
| 3.5 | .637 | 5° | 8.9° | 21 | 1.6 |
| 4 | .637 | 5° | 8.9° | 28 | 1.4 |
| 4.5 | .637 | 6° | 10.7° | 29 | 1.3 |

V-coupler and DRG that gives minimum $L$. The minimum coupling loss achievable as a function of $a/b$ (with optimum $l$, $\theta$, and $\Delta\theta$, and with the desired driving-point impedance) is shown in Fig. 9. The designs for the corresponding couplers are given in Table II. The coupling improves substantially as $a/b$ increases from two to four, but improvement slows for $a/b > 4$. As pointed out earlier, increasing $a/b$ tends to decrease the mechanical strength of the waveguide. Considering this tradeoff, $a/b = 4$ appears to be a good choice.

## IV. CONCLUSION

We have shown that for a good design, a coupling loss on the order of 1.4 dB can be expected between dielectric ridge guide and a small device connected at the vertex of a V-coupler. To this must be added dielectric losses and

ohmic losses in the V-coupler at the millimeter-wave frequency. For the case of 1000-Ω·cm silicon, one expects dielectric loss of the order of 0.5 dB/cm (nearly independent of frequency)[1]. In earlier work at 85 GHz, ohmic loss in the V-coupler was found to be about 1.2 dB [21]. Thus, one can expect to couple radiation from free space, through a centimeter of guide, and into a correctly matched device with an overall coupling loss of slightly more than 3 dB. This loss is small enough to make DRG an interesting component for millimeter-wave integrated circuits, particularly at the higher frequencies where hollow waveguides are inconvenient and metallic losses are severe.

## References


[1] E. A. J. Marcatili, "Dielectric rectangular waveguide and directional coupler for integrated optics," *Bell Syst. Tech. J.*, vol. 48, pp. 2071–2102, Sept. 1969.

[2] J. E. Goell, "A circular-harmonic computer analysis of rectangular dielectric waveguides", *Bell Syst. Tech. J.*, vol. 48, pp. 2133–2160, Sept. 1969.

[3] R. M. Knox and P. P. Toulios, "Integrated circuits for the millimeter through optical frequency range", in *Proc. Symp. Submillimeter Waves*, (New York, NY), Mar. 1970, pp. 497–516.

[4] P. P. Toulios and R. M. Knox, "Image line integrated circuits for system applications at millimeter wavelengths." U.S. Army Electronics Command, Final Rep., Dept. no. ECOM-73-0217-F, July 1974.

[5] K. Solbach and I. Wolff, "The electromagnetic fields and the phase constants of dielectric image lines," *IEEE Trans. Microwave Theory Tech.*, vol. MTT-26, pp. 266–274, Apr. 1978.

[6] T. Itoh and R. Mittra, "New waveguide structures for millimeter-wave integrated circuits," in *Int. Microwave Symp. Dig.*, May 1975, pp. 277–279.

[7] W. V. McLevige, T. Itoh, and R. Mittra, "New waveguide structures for millimeter wave and optical integrated circuits," *IEEE Trans. Microwave Theory Tech.*, vol. MTT-23, pp. 788–794, Oct. 1975.

[8] T. Itoh, "Inverted strip dielectric waveguide for millimeter wave integrated circuits," *Trans. Microwave Theory Tech.*, vol. MTT-24, pp. 821–827, Nov. 1976.

[9] R. Mittra, Y-L. Hou, and V. Jamnejad, "Analysis of open dielectric waveguides using mode-matching technique and variational methods," *IEEE Trans. Microwave Theory Tech.*, vol. MTT-28, pp. 36–43, Jan. 1980.

[10] T. Itoh and B. Adelseck, "Trapped image guide for millimeter-wave circuits," *IEEE Trans. Microwave Theory Tech.*, vol. MTT-28, pp. 1433–1436, Dec. 1980.

[11] S.-T. Peng and A. A. Oliner, "Guidance and leakage properties of a class of open dielectric waveguides: Part I—Mathematical formulations," *IEEE Trans. Microwave Theory Tech.*, vol. MTT-29, pp. 843–855, Sept. 1981.

[12] A. A. Oliner, S-T. Peng, T. I. Hsu, and A. Sanchez, "Guidance and leakage properties of a class of open dielectric waveguides: Part II—New physical effects," *IEEE Trans. Microwave Theory Tech.*, vol. MTT-29, pp. 855–869, Sept. 1981.

[13] H. Jacobs and M. M. Chrepta, "Electronic phase shifter for millimeter-wave semiconductor dielectric integrated circuits," *IEEE Trans. Microwave Theory Tech.*, vol. MTT-22, pp. 411–417, Apr. 1974.

[14] D. B. Rutledge, S. E. Schwarz, T.-L. Hwang, D. J. Angelakos, K. K. Mei, and S. Yokota, "Antennas and waveguides for far-infrared integrated circuits," *IEEE J. Quantum Electronics*, vol. QE-16, pp. 508–516, May 1980.

[15] J. G. Gallagher, "Mode dispersion of trapezoidal cross-section dielectric optical waveguides by the effective-index method," *Electron. Lett.*, vol. 15, no. 23, pp. 734–735, Nov., 1979.

[16] E. A. J. Marcatili, "Bends in optical dielectric guides," *Bell Syst. Tech. J.*, vol. 48, pp. 2103–2132, Sept. 1969.

[17] E. A. J. Marcatili and S. E. Miller, "Improved relations describing directional control in electromagnetic wave guidance," *Bell Syst. Tech. J.*, vol. 48, pp. 2161–2188, Sept. 1969.

[18] K. Solbach, "The measurement of the radiation losses in dielectric image line bends and the calculation of a minimum acceptable curvature radius," *IEEE Trans. Microwave Theory Tech.*, vol. MTT-27, pp. 51–53, Jan. 1979.

[19] D. B. Rutledge, S. E. Schwarz, and A. T. Adams, "Infrared and submillimeter antennas," *Infrared Phys.*, vol. 18, pp. 713–729, 1978.

[20] J. Galejs, *Antennas in Inhomogeneous Media*. Oxford: Pergamon Press, 1969.

[21] C. Yao, S. E. Schwarz, and B. J. Blumenstock, "Monolithic integration of a dielectric millimeter-wave antenna and mixer diode: An embryonic millimeter-wave IC," *IEEE Trans. Microwave Theory Tech.*, vol. MTT-30, pp. 1241–1247, Aug. 1982.


[1]This estimate is based on the dc conductivity. Anomalous loss mechanisms can be expected to appear at higher frequencies.


**Taichi Wang** (S'78) was born in Taipei, Taiwan, on November 13, 1955. He received the B.A. degree in physics from the University of California, Irvine, in 1978, and the M.S. degree in applied physics from the University of California, San Diego, in 1979. Since 1980 he has been working toward the Ph.D. degree in electrical engineering in the Department of Electrical Engineering and Computer Science, University of California, Berkeley. His research interests are in electromagnetic theory, semiconductor devices, and millimeter-wave integrated circuits.

**S. E. Schwarz** (SM'71) was born in Los Angeles, CA, on January 29, 1939. He received the B.S. degree in physics from California Institute of Technology in 1959, the A.M. in physics from Harvard University in 1961, and the Ph.D. in electrical engineering from Caltech in 1964.

He has held positions with Hughes Research Laboratories, Bell Laboratories, and IBM Research Laboratories. Since 1964 he has been a member of the faculty of Electrical Engineering and Computer Sciences at the University of California, Berkeley, where he is engaged in work on millimeter-wave devices and integrated circuits and quantum electronics.

Prof. Schwarz held a Guggenheim Fellowship in 1971–1972. He is co-author of the textbook *An Introduction to Electronics* and of *Electrical Engineering: An Introduction*, to appear in 1983.